InAs on InP: Intermediate alloy formation and interface vibrations

Lucia G. Quagliano

I.M.A.I.-C.N.R., Area della Ricerca di Roma, P.O. Box 10, via Salaria km 29.300, 00016 Monterotondo Scalo, Roma, Italy

Bernard Jusserand

C.N.E.T., Laboratoire de Bagneux, 196 Avenue H. Ravera, 92220 Bagneux, France

Daniela Orani

I.M.A.I.-C.N.R., Area della Ricerca di Roma, P.O. Box 10, via Salaria km 29.300, 00016 Monterotondo Scalo, Roma, Italy

We present a detailed investigation of the vibrational modes of single thin InAs layers directly grown on InP substrate. The Raman spectra have revealed the presence of features besides the longitudinal-optical and transverse-optical modes related to InP and InAs. We have succeeded in distinctly detecting Raman modes due to the presence of an intermixed $In_xAs_{1-x}P$ layer resulting from an incorporation of arsenic in the InP substrate. Moreover, our Raman data show unusual intense features related to the lattice vibrations of interface bonds. The observed energies of these interface modes are in good agreement with the calculation based on a modulated dielectric model. This work clearly demonstrates that the vibrational properties of heterostructures can be sensitive to the structure of the interface and that Raman spectroscopy is a powerful tool to investigate the crystal structure of heterostructures as well as the interfacial chemistry. [S0163-1829(97)02932-9]

I. INTRODUCTION

In recent years increasing interest has been focused on InAs/InP strained layer systems because they are relevant to optoelectronic applications in the near IR. The high electron mobilities in InAs have significant potential for high-mobility electron device applications. An important and crucial aspect of the device application is the interface quality. Raman spectroscopy is a very powerful technique to probe the lattice vibration of solids. In particular, this technique is very sensitive to the interface roughness or intermixing and is useful for characterizing the local structure of interfaces.

Only a few reports on Raman studies of vibrations in InAs/InP single quantum wells have been published.[1-3] In these reports Raman lines related to InAs vibrations have been analyzed in order to determine confinement and strain effects in these materials. In Ref. 3 additional bands, attributed to interface phonons, have been observed between the transverse-optical (TO) and longitudinal-optical (LO) lines of both InAs and InP.

In this paper we present a Raman study of vibrational properties of individual and ultrathin layers of InAs directly grown on InP (001) substrates, without a cap layer. The Raman spectra have revealed several new structures in addition to the LO and TO modes related to InAs and InP: (i) broadbands between TO and LO phonons of InAs and InP; (ii) intense narrow features close to the bulk optical phonons of InAs and InP. Owing to a detailed experimental study of the intensities and frequencies of these phonon modes as a function of the incident wavelength as well as of InAs thickness, we have assigned the broadbands to interfacial alloy vibrations and the narrow lines to the interface (IF) phonons of the structure. These assignments differ from the one reported in Ref. 3, where all additional lines have been analyzed in terms of interface phonons without any reference to an inter-

face alloy. In order to evaluate the nature and the frequencies of the observed modes, the experimental data have been compared with a calculation based on the modulated dielectric model. To have a realistic description of the modes we have included an interfacial layer of $In_xAs_{1-x}P$ in the calculation. Good agreement between experiments and theory has been obtained.

We would like to point out that one important result of this work is the experimental evidence of the presence of the strained $In_xAs_{1-x}P$ interlayer, probably due to a reactive substitution of P atoms by As during the thermal cleaning of the InP substrate under arsenic pressure.

II. EXPERIMENT

A series of single layers of InAs, with a nominal thickness 3–9 ML, has been grown by molecular-beam epitaxy (MBE) directly on InP substrates. The layer thicknesses have been estimated from the bulk growth rates. Epitaxial growth has been carried out in a solid-source MBE system and has been monitored *in situ* by reflection high-energy electron diffraction (RHEED).

The substrates were semi-insulating (001) oriented wafers of "ready to use" quality. Prior to growth, the substrate surface was thermally cleaned under an arsenic flux of about 1×10^{-5} Torr at a substrate temperature of about 520 °C. The heating was interrupted on the appearance of a clearly 2×4 reconstruction observed in the RHEED pattern, indicative of oxide removal from the InP. After this standard cleaning and oxide desorption procedure the substrate temperature was decreased to 380 °C and InAs layers were grown.

The Raman experiments were performed at 80 and 300 K using two different excitation wavelengths: 476.5 nm (2.61 eV) and 514.5 nm (2.41 eV). The Raman scattering light was analyzed with a DILOR Modular XY-Laser Raman spec-
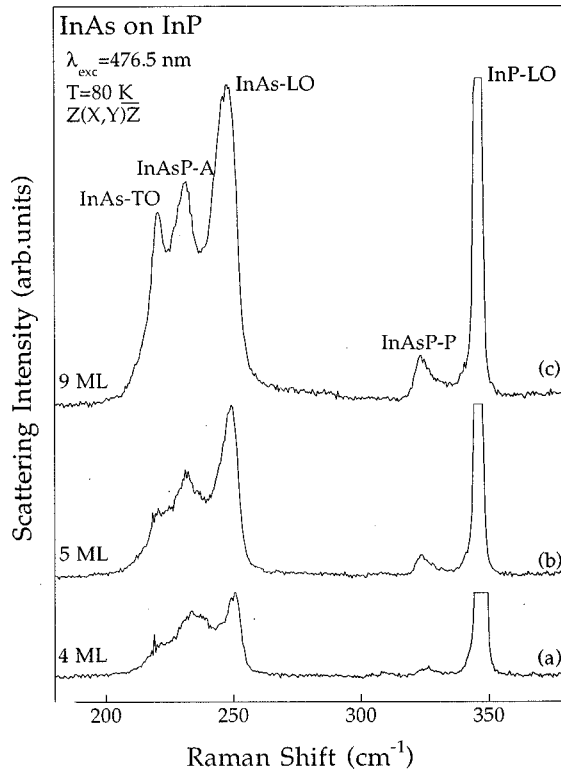
FIG. 1. Raman spectra measured at 80 K with an excitation wavelength of 476.5 nm for the samples with nominal InAs thickness: (a) 4 ML, (b) 5 ML, and (c) 9 ML. Data were collected in the $Z(X,Y)\overline{Z}$ configuration.

trometer system and detected with a nitrogen-cooled charge-coupled device. The spectra were recorded in quasibackscattering geometry from the (001) growth surface with the $Z(X,Y)\overline{Z}$ and $Z(X,X)\overline{Z}$ configurations; X, Y, and Z are defined along the (001), (010), and (001) crystal axes, respectively.

III. RESULTS AND DISCUSSION

Figures 1(a)–1(c) show Raman spectra for the samples with a nominal thickness $d=4$, 5, and 9 ML. The spectra were measured at 80 K with an excitation wavelength of 476.5 nm. This laser line was selected because of the resonance enhancement of the Raman signal at the E_1 band-gap energy of bulk InAs.[4] The data were recorded in backscattering geometry in the $Z(X,Y)\overline{Z}$ configuration. As expected from a (001) oriented sample, in this perpendicular configuration scattering by LO phonons is allowed according to the symmetry selection rules, whereas scattering from TO phonons is forbidden. The observed Raman spectra show several peaks. The LO-phonons mode from InP substrate at $\cong 346$ cm^{-1} as well as the LO-phonon mode relative to the InAs layer around $\cong 249$ cm^{-1} are the dominant peaks. The weaker peak in the low-frequency side of the spectra at $\cong 221$ cm^{-1} could be assigned to the InAs TO-phonon mode which is symmetry forbidden in this configuration. Its activation should be due to departure from exact backscattering and/or to crystal imperfections. The peak positions of the InAs LO phonon are shifted towards higher energies with respect to the bulk phonon value ($\cong 7$ cm^{-1}) and its fre-

quency does not depend significantly on the thickness between 3 and 9 ML. This shift is reasonably explained by the effect of compressive strain in the InAs layer given by the large lattice mismatch ($\cong 3.2\%$) between InAs and InP. The estimated value of this shift, deduced from textbook values of the elastic parameters,[5] is $\cong 10$ cm^{-1}. However, we cannot exclude some contribution due to a slight strain relaxation and to phonon confinement.

Besides these modes, different features have been observed in the Raman spectra. These structures positioned between bulk InP and InAs optical energies are attributed to the presence of a mixed In$_x$As$_{1-x}$P layer. This ternary compound is formed on the InP substrate because of the unintentional incorporation of arsenic during the thermal cleaning of InP surface.[6,7] As a matter of fact, thermal desorption of surface oxide from InP (001) requires heating well above the congruent evaporation temperature, implying decomposition and a severe loss of phosphorus that is replaced by arsenic. The In$_x$As$_{1-x}$P alloy, like most ternary compounds, exhibits a two-mode vibrational spectrum over the whole composition range. This means that the scattering from optical phonons exhibits two bands, one close to the frequency of pure InP and the other near the pure InAs. Therefore, the lines observed at $\cong 324$ and $\cong 232$ cm^{-1} are assigned to InP-like (In$_x$As$_{1-x}$P-P) and InAs-like (In$_x$As$_{1-x}$P-A) vibrations of the additional In$_x$As$_{1-x}$P interfacial layer, respectively. The energies of these modes do not shift with increasing InAs thickness. As the lattice constant of In$_x$As$_{1-x}$P is bigger than that of InP, this alloy is expected to be under biaxial compressive strain causing a shift of LO-phonon lines to higher frequencies. A quantitative estimate of the alloy composition of this intermixed layer from the position of the phonon modes is difficult to obtain because it is necessary to know the concentration profile and the strain distribution of this interfacial layer. Our results indicate that phosphorus on the top of the InP substrate was replaced by arsenic during the surface passivation, resulting in the formation of an In$_x$As$_{1-x}$P layer. Therefore, in thin InAs films grown on InP substrate one expects an In$_x$As$_{1-x}$P interfacial layer immediately adjacent to the InAs layer and these systems can be described by a three-layers model InAs/In$_x$As$_{1-x}$P/InP. These results are in agreement with recent observations obtained from x-ray photoelectron diffraction measurements[7] and selected area x-ray photoelectron spectroscopy.[6]

In Figs. 2(a)–2(c) we present Raman spectra for the same samples reported in Fig. 1. These spectra were measured at the same temperature and excitation energy, but they were collected in the $Z(X,X)\overline{Z}$ scattering configuration. When the polarization of the scattered light is parallel to that of the incident light, the LO-phonon scattering by the deformation-potential mechanism is symmetry forbidden.[8] Therefore, the Raman activity of the LO phonons is considerably reduced in comparison with the spectra taken in the $Z(X,Y)\overline{Z}$ configuration and is only due to the Fröhlich mechanism. Because this mechanism is effective only at resonance, the InP LO is drastically reduced in intensity in this configuration. On the contrary, because of the E_1 resonance, the phonons relative to InAs are less reduced in parallel configuration; in particular, the LO phonon from InAs is the prominent feature. Forbidden scattering from InAs TO phonon is still observed under this scattering configuration.
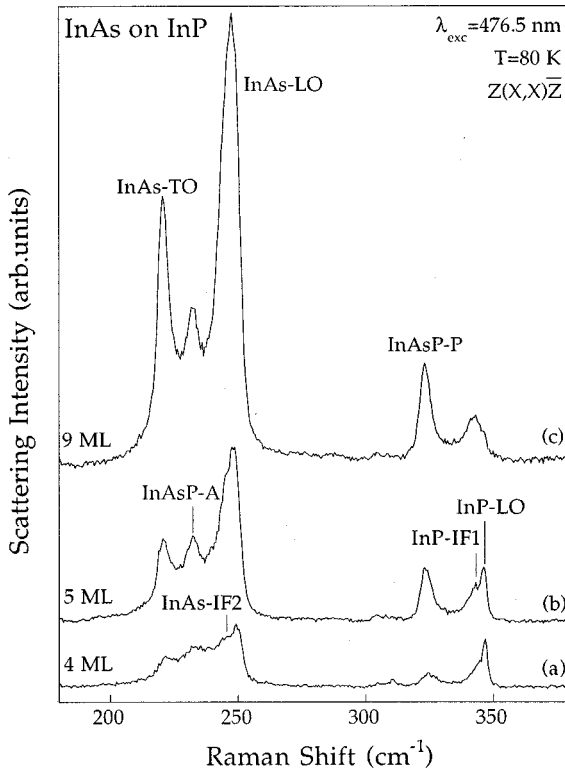
FIG. 2. Raman spectra measured at 80 K with an excitation wavelength of 476.5 nm for the samples with nominal InAs thickness: (a) 4 ML, (b) 5 ML, and (c) 9 ML. Data were collected in the $Z(X,X)\overline{Z}$ configuration. Peaks denoted by IF are interface-related phonons.
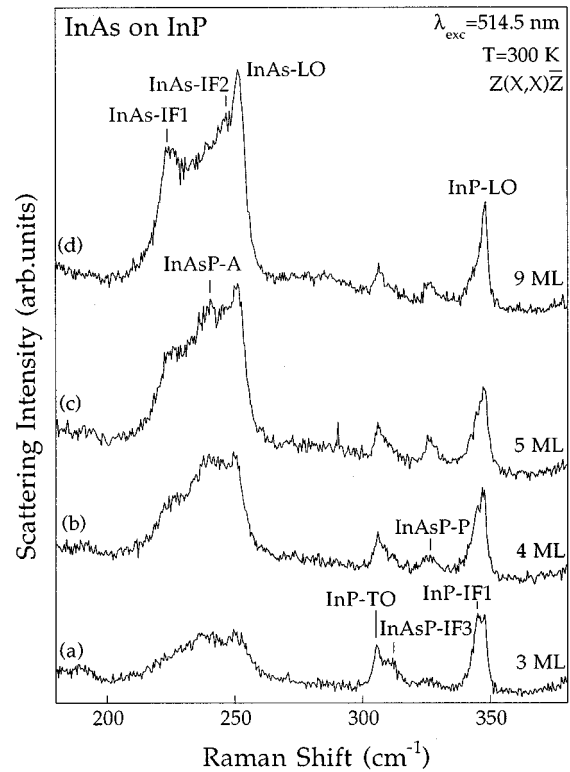
FIG. 3. Room-temperature Raman spectra measured using the 514.5-nm excitation wavelength for the samples with nominal InAs thickness: (a) 3 ML, (b) 4 ML, (c) 5 ML, and (d) 9 ML. The spectra were recorded in the $Z(X,X)\overline{Z}$ configuration. Peaks denoted by IF are interface-related phonons.

In Figs. 3(a)–3(d) we present typical Raman spectra from the samples with nominal thickness $d=3$, 4, 5, and 9 ML. The spectra have been obtained at room temperature in the $Z(X,X)\overline{Z}$ configuration with an excitation wavelength of 514.5 nm. In these conditions we are no longer close to the resonance with the E_1 gap energy of the bulk InAs. In the figure, as in the previous one, several additional lines are observed besides the TO and LO peaks. We assign all these lines to modes related to interface phonons. A calculation of their frequencies based on a modulated dielectric model will be presented after. To simplify the description of the spectra displayed in Figs. 2 and 3, we can anticipate from the result of the calculation that there are seven different interface phonons in the structure: one InP-like, four $In_xAs_{1-x}P$-like, and two InAs-like. In the InP region of the experimental spectra, we observe a weak LO-phonon signal and in addition to this mode a well-resolved peak which is assigned to scattering by InP interface mode (InP-IF1). The strength of this mode decreases with increasing thickness of the InAs. For the sample with 3 ML this interface mode is comparable to the LO mode of InP substrate. Besides, the Raman spectra present two peaks close to the InP TO energy. The lowest-energy one is attributed to the InP TO-phonon mode, the other one decreases in intensity with respect to the InP LO-phonon mode with increasing InAs thickness. We ascribe the latter to an interface phonon mode of the $In_xAs_{1-x}P$ alloy related to the interface with the InP substrate ($In_xAs_{1-x}P$-IF3). The other interface mode of the alloy related to the interface with InP ($In_xAs_{1-x}P$-IF4) is not ob-

served. We believe that it is not resolved from the InP-type LO-phonon mode of the alloy ($In_xAs_{1-x}P$-P).

Concerning the InAs phonon region, the Raman spectra in Fig. 3 exhibit significant changes compared to the spectra reported in Fig. 2 which have been obtained in the same parallel configuration but under resonant excitation conditions. Changing the excitation energy and the sample temperature we are no longer close to resonance with the E_1 gap energy of InAs and the LO-phonon line relative to InAs is drastically reduced in intensity. On its low-energy side a different structure has been observed, which we assign to the interface mode between InAs and $In_xAs_{1-x}P$ (InAs-IF2). Close to the TO frequency of InAs, we have observed a line which could correspond to both the InAs TO mode and the surface mode of InAs (InAs-IF1). We have also observed a broadband, positioned around 235 cm^{-1}, in the energy range of the InAs-type modes of the $In_xAs_{1-x}P$ alloy. This band is due to the overlapping of the interface modes $In_xAs_{1-x}P$-IF1 and $In_xAs_{1-x}P$-IF2 with the bulk vibrations. In our opinion, these modes are not resolved because of the proximity of their frequencies, combined with alloy broadening.

Comparing the spectra presented in Fig. 3 with the corresponding spectra in Figs. 2 and 1 we note that in resonance conditions the InP-IF1, $In_xAs_{1-x}P$-A and $In_xAs_{1-x}P$-P modes increase in intensity with the InAs-deposited thickness. In these conditions the contribution of the $In_xAs_{1-x}P$ layer is probably also selectively enhanced. For instance, the InP-IF1 mode (localized at the interface between InP and $In_xAs_{1-x}P$) is mostly Raman active thanks to its extension
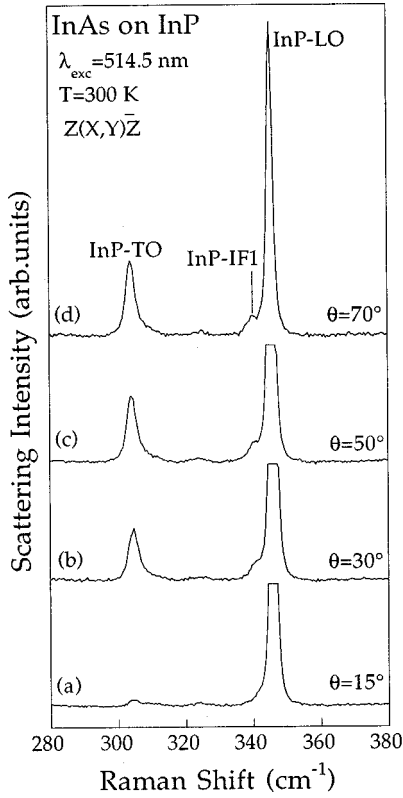
FIG. 4. Room-temperature Raman spectra measured using the 514.5-nm excitation wavelength in the $Z(X,Y)\overline{Z}$ configuration for the sample with nominal thickness 6 ML for different value of the scattering angle: (a) 15°, (b) 30°, (c) 50°, and (d) 70°.

within $\text{In}_x\text{As}_{1-x}\text{P}$ which likely increases with the InAs-deposited thickness. For a more quantitative understanding of these variations we should have at least the exact value of the E_1 transitions in the surface layers. Probably these values display some variations as a function of the deposited thickness and modify the Raman activity of the corresponding phonons.

Figure 4 shows Raman spectra of the 6-ML sample obtained in perpendicular configuration for different incident angles of the laser beam at the same temperature and excitation energy of the spectra reported in Fig. 3. Varying the angle θ between the directions of the incident and scattered light a range of in-plane wave vectors has been generated. The intensity of the InP TO line increases with increasing angle in the Raman spectrum because of the change of the selection rules due to the departure from the exact (001) orientation. Moreover, a new peak is clearly observed on the low-frequency side of the LO-phonon from InP. With increasing incident angle from the backscattering geometry this mode becomes more distinct. In quasibackscattering configuration the in-plane wave vector k_x transferred to the phonon is small. Therefore, the frequencies of the IF phonons are close to the frequencies of the LO phonons and we have observed them only in parallel configuration where the LO lines are weak. With increasing k_x the frequency of the IF phonon shifts away from the LO frequency and this peak related to the interface phonon localized at the boundary between the InP substrate and the $\text{In}_x\text{As}_{1-x}\text{P}$ layer (InP-IF1) becomes observable in the crossed configuration. This confirms our assignment of the peaks observed beside the
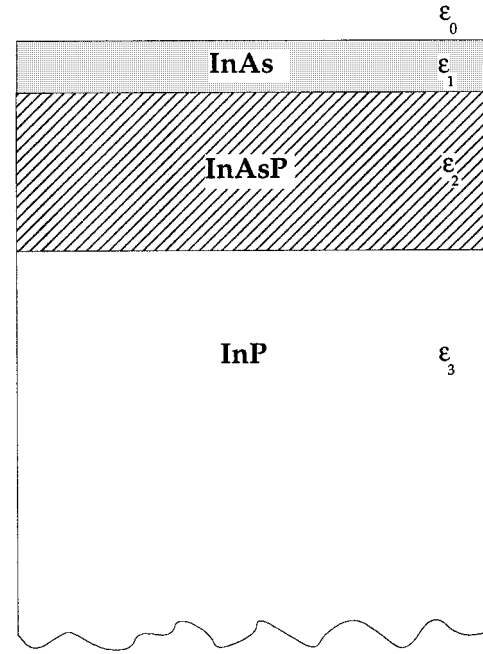

FIG. 5. Schematic representation of the semi-infinite three-layer system ($i=1,2,3$) in contact with the vacuum ($i=0$).

LO and TO modes of InP and InAs as modes related to the interfaces.

In order to get a quantitative description of these interface modes, we have performed a calculation within the modulated dielectric model. We have modified the calculation introduced by Nakayama, Ishida, and Sano[9] in order to include the strained interfacial alloy. We have considered a semi-infinite multilayer system $\text{InP}/\text{In}_x\text{As}_{1-x}\text{P}/\text{InAs}/\text{vacuum}$, schematically depicted in Fig. 5. Each constituent is characterized by a local dielectric constant $\varepsilon(\omega)$:

$$\varepsilon_i = 1 \quad \text{for } i=0, \tag{1}$$

with $i=0$ standing for vacuum;

$$\varepsilon_i = \varepsilon_\infty^i \frac{\omega^2 - \omega_{\text{LO}_i}^2}{\omega^2 - \omega_{\text{TO}_i}^2} \quad \text{for } i=1 \quad \text{and } i=3, \tag{2}$$

with $i=1,3$ corresponding to InAs and InP, respectively. ε_∞ denotes the high-frequency dielectric constant, ω_{LO} and ω_{TO} are the longitudinal and transverse-optical-phonon frequency of the InAs and InP layers;

$$\varepsilon_i = \varepsilon_\infty^2 \frac{\omega^2 - \omega_{\text{LO}_{2A}}^2}{\omega^2 - \omega_{\text{TO}_{2A}}^2} \times \frac{\omega^2 - \omega_{\text{LO}_{2P}}^2}{\omega^2 - \omega_{\text{TO}_{2P}}^2} \quad \text{for } i=2, \tag{3}$$

with $i=2$ corresponding to $\text{In}_x\text{As}_{1-x}\text{P}$ alloy which exhibits a two-mode behavior; $\omega_{\text{LO}_{2A}}$, $\omega_{\text{TO}_{2A}}$ and $\omega_{\text{LO}_{2P}}$, $\omega_{\text{TO}_{2P}}$ standing for the InAs-like and InP-like, respectively.

The parameters of these materials are listed in Table I. We have used textbook values for InP and InAs, modified to take into account the effect of strain. Concerning the $\text{In}_x\text{As}_{1-x}\text{P}$ alloy, its phonon frequencies are known with a limited accuracy[10] and, to our knowledge, their strain dependence is not available. We have roughly estimated the As concentration to be $(50\pm10\,\%)$ and we have used in the

TABLE I. Transverse- and longitudinal-phonon frequencies, high-frequency dielectric constants and thicknesses of InAs, InP, and In$_x$As$_{1-x}$P alloy.

	ω_{TO} (cm^{-1})	ω_{LO} (cm^{-1})	ε_∞	d (nm)	i
InAs	228	252	11.8	2	1
InP	304	346	9.5		3
In$_x$As$_{1-x}$P (InAs-like)	232 ($\omega_{TO_{2A}}$)	241 ($\omega_{LO_{2A}}$)	10.7	10	2
In$_x$As$_{1-x}$P (InP-like)	315 ($\omega_{TO_{2P}}$)	334 ($\omega_{LO_{2P}}$)	10.7	10	2

calculation the values of Carles *et al.*[10] at this concentration, shifted by 5 cm^{-1} that is half of the predicted strain shift in the InAs layer.

The dispersion relation of the interface modes in the infinite three-layer system can be obtained from Maxwell's equations together with conventional boundary conditions. By using the above-defined notations we have obtained

$$\left(1-\frac{k_2\varepsilon_3}{k_3\varepsilon_2}\right)\left[\left(1-\varepsilon_1\frac{k_0}{k_1}\right)\left(1+\frac{k_1\varepsilon_2}{k_2\varepsilon_1}\right)+\exp(-2k_1d_1)\right.$$
$$\times\left(1+\varepsilon_1\frac{k_0}{k_1}\right)\left(1-\frac{k_1\varepsilon_2}{k_2\varepsilon_1}\right)\right]+\exp(-2k_2d_2)\left(1+\frac{k_2\varepsilon_3}{k_3\varepsilon_2}\right)$$
$$\times\left[\left(1-\varepsilon_1\frac{k_0}{k_1}\right)\left(1-\frac{k_1\varepsilon_2}{k_2\varepsilon_1}\right)+\exp(-2k_1d_1)\left(1+\varepsilon_1\frac{k_0}{k_1}\right)\right.$$
$$\times\left(1+\frac{k_1\varepsilon_2}{k_2\varepsilon_1}\right)\right]=0, \qquad (4)$$

with

$$k_{iz}=\left[k_x^2-\varepsilon_i(\omega)\left(\frac{\omega^2}{c^2}\right)\right]^{1/2}, \qquad (5)$$
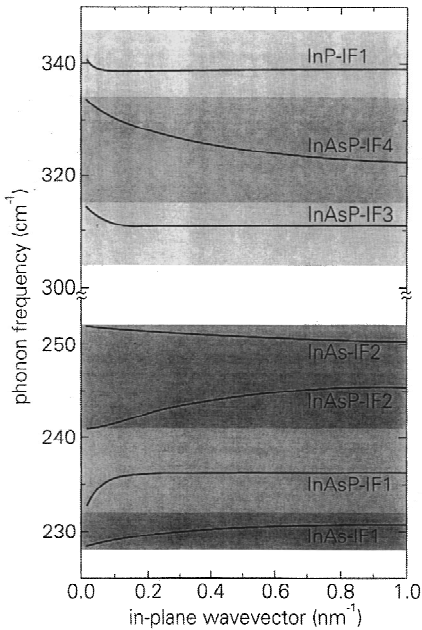

FIG. 6. Theoretical dispersion curves of the interface modes calculated within the modulated dielectric model. The areas filled with light gray, gray, and dark gray show the TO-LO ranges of the bulk compounds InP, In$_x$As$_{1-x}$P, and InAs, respectively.

where k_{iz} corresponds to the z component of the wave vector in individual layers; k_x is the x component with x the direction parallel to interfaces, which is constant over the whole structure; c is the speed of propagation of light; d_1 and d_2 are the thicknesses of the InAs and In$_x$As$_{1-x}$P layers, respectively.

The interface modes in our system are the solutions of Eq. (4), which has been solved numerically. In Fig. 6 we show the theoretical dispersion curves of these modes. The inclusion of the In$_x$As$_{1-x}$P alloy with its two-mode behavior gives rise to a new situation because the alloy-related oscillators are included within the reststrahlen bands of the other layers. The resulting in-plane dispersion curve is qualitatively different from the one previously published by Nakayama[9] and we observe seven modes instead of four. Two of them, In$_x$As$_{1-x}$P-IF2 and IF3, exhibit opposite in-plane dispersion with respect to the normal behavior. These dispersion curves allow us to assign most of the peaks observed in the spectra, some of them appearing for particular experimental configurations. We believe that these peaks could arise from the activation of large k_x interface phonons. The observation of these modes requires an additional scattering mechanism in the Raman process. We suggest that one possible explanation of the origin of this scattering could derive from interface roughness. The presence of the ternary In$_x$As$_{1-x}$P is very likely to be responsible for interface disorder and this could provide the relaxation of the parallel momentum conservation and the activation of the IF modes. The effect of this activation can be seen in Fig. 7 where we have attempted to model the contribution of interface modes to the Raman spectra. Contrary to the experimental results, in this figure there is not the contribution of the bulk phonons. Using a Lorentzian wave-vector relaxation with a half width
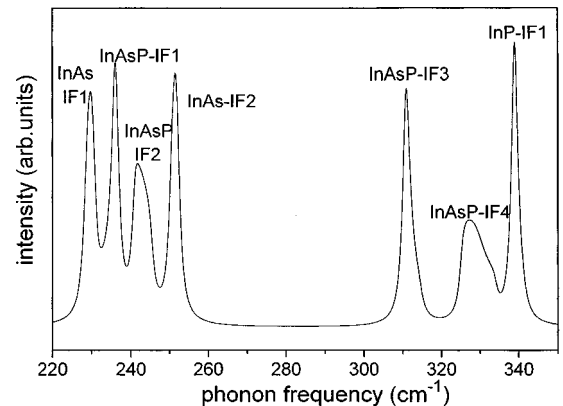

FIG. 7. Spectral density of interface phonon modes, calculated for vanishing average in-plane wave vector and a Lorentzian broadening with a half width of $\cong 0.25$ nm^{-1}.

of 0.25 nm^{-1}, we have obtained seven structures peaked at the interface frequencies, providing a good qualitative description of the observed peaks, particularly in the InP energy region. Among the seven interface modes predicted in our calculation, four of them are well resolved in the experiments: InP-IF1, In$_x$As$_{1-x}$P-IF3, InAs-IF2, and perhaps InAs-IF1. We believe that the other peaks (In$_x$As$_{1-x}$P-IF1, In$_x$As$_{1-x}$P-IF2, In$_x$As$_{1-x}$P-IF4) are not resolved because the individual mode frequencies are superimposed to the bulk modes of the alloy which are broadened by the disorder and/or by some composition variation not considered in the model. From this quantitative analysis we deduce that, because of the introduction of the alloy, the interface modes become very close to the bulk phonon modes and weakly dispersive as a function of the in-plane wave vector. Contrary to Ref. 3, we do not need to introduce two different wave vector ranges to explain all the new lines from the interface phonon dispersion.

We would like to point out that our quantitative model well supports the description of the InAs/InP Raman spectra presented in this work, including the contribution of both intermediate alloy vibrations and disorder-activated interface phonons of the whole structure.

IV. CONCLUSION

We have investigated by Raman spectroscopy the interface of InAs/InP heterostructures, with an InAs layer thickness between 3 and 9 ML. The Raman spectra have shown, in addition to the peak structures due to the LO and TO phonons related to InP and InAs, two different features: (i) broadbands between TO and LO phonons of InAs and InP,

(ii) intense narrow features close to the bulk optical phonons of InAs and InP. We have attributed the broadbands to interfacial alloy vibrations due to the presence of an interfacial In$_x$As$_{1-x}$P layer between InP and InAs. This ternary compound is due to the unintentional incorporation of arsenic on InP substrate during the thermal cleaning of the substrate under an arsenic pressure before the growth of InAs layers. Concerning the intense features appearing just below the bulk optical-phonon energies, their intensities and line shapes depend on the angle between the directions of the incident and scattered beams. From this behavior and from the positions of the peaks, we deduce that they are related to the lattice vibrations of interface bonds. We have attributed these modes to interface phonons and analyzed their frequencies by using a modulated dielectric model, which provides a good qualitative description of the experimental spectra.

We have been able to observe Raman scattering coming from a very small amount of scattering species thanks to the use of specific excitation wavelengths close to electronic resonances of the surface layers. This study demonstrates that Raman scattering is not only sensitive to the thin layer at the surface but provides detailed quantitative information on the vibrational structure of complex stackings which takes place during the first stage of heteroepitaxy of semiconductors.

[1] L. Pavesi, G. Mariotto, J. F. Carlin, A. Rudra, and R. Houdré, Solid State Commun. **84**, 705 (1992).

[2] J. Groenen, A. Mlayah, R. Carles, A. Ponchet, A. Le Corre, and S. Salaun, Appl. Phys. Lett. **69**, 943 (1996).

[3] C. A. Tran, J. L. Brebner, R. Leonelli, M. Jouanne, and R. A. Masut, Phys. Rev. B **49**, 11 268 (1994).

[4] R. Carles, N. Saint-Cricq, J. B. Renucci, A. Zwick, and M. A. Renucci, Phys. Rev. B **22**, 6120 (1980).

[5] B. Jusserand and M. Cardona, *Light Scattering in Solids V*, edited by M. Carona and G. Guentherodt (Springer, Berlin, 1989), p. 49.

[6] M. R. Bruni, N. Gambacorti, S. Kaciulis, G. Mattogno, M. G. Simeone, L. G. Quagliano, N. Tomassini, and B. Jusserand, J. Cryst. Growth **150**, 123 (1995).

[7] E. Bergignat, M. Gendry, G. Hollinger, and G. Grenet, Phys. Rev. B **49**, 13 542 (1994).

[8] M. Cardona, *Light Scattering in Solids II*, edited by M. Cardona and G. Guentherodt (Springer, Berlin, 1982), p. 19.

[9] M. Nakayama, M. Ishida, and N. Sano, Phys. Rev. B **38**, 6348 (1988).

[10] R. Carles, N. Saint-Cricq, J. B. Renucci, and R. J. Nicholas, J. Phys. C **13**, 899 (1980).